Talanta 82 (2010) 555–559

Contents lists available at ScienceDirect

Talanta

journal homepage: www.elsevier.com/locate/talanta

Cavity microelectrode for studying manganese dioxide powder as pH sensor

Christine Cachet-Vivier[a,*], Bernard Tribollet[b], Vincent Vivier[b]

[a] Électrochimie et Synthèse Organique, Institut de Chimie et Matériaux Paris Est, CNRS, Université Paris Est Créteil, 2-8 rue H. Dunant, 94320 Thiais, France
[b] Laboratoire Interfaces et Systèmes Électrochimiques, UPR 15 du CNRS, Université Pierre et Marie Curie, 4 place Jussieu, CP133, 75252 Paris Cedex 05, France

ARTICLE INFO

Article history:
Received 13 November 2009
Received in revised form 24 April 2010
Accepted 10 May 2010
Available online 27 May 2010

Keywords:
MnO_2
pH microsensor
Cavity microelectrode

ABSTRACT

The potential–pH response of an electrolytic manganese dioxide is investigated by means of a cavity microelectrode (CME). The potential–pH curves show a complex evolution that could be explained by the disporportionation of MnOOH species, leading to the formation of Mn^{2+} ions on the MnO_2 surface. Such a behaviour is not suited for pH sensor application. However when the tip of the electrode is coated by a Nafion membrane, the potential–pH evolution shows a unique slope close to $-60\,mV\,pH^{-1}$. In addition, the sensor exhibits short time responses to pH variations, a good selectivity, and it can be easily renewed compared to classical sensors.

1. Introduction

The development of pH microelectrode for local measurements is of the greatest importance for biologic, environmental or corrosion applications [1–7]. Many types of commercial pH microelectrodes are actually available such as glass membrane microelectrodes, liquid-ion exchanger electrodes and solid-state electrodes. The choice of the electrode technology depends on the specific requirements of each experiment and sensor properties such as sensitivity, accuracy of measurement, working range, response time, calibration and/or offset correction, long time stability providing guidance for selecting the best sensors. For instance, commercial glass microelectrodes and liquid-ion exchanger electrodes are increasingly common use; however, they are not suited for near field microscopy techniques because of the fragility of the former system and the short span of life (usually less than one day) of the latter. Other types of pH microsensors have been devised such as hydrogel base pH microsensors [8], pH IFSET microsensors [9], optical fiber pH microsensors [10] and significant efforts have been made to develop all solid-state devices and in particular metal oxide-based electrodes. Among the different metal oxides investigated, iridium oxide (IrO_x) appears to be one of the most promising material [11–16]; its main advantages being a wide linear pH-response, a fast and stable time response, a long time stability in various electrolyte such as in aqueous and corrosive solutions over a wide range of temperature and pressure, and a low dependence to interfering ions. These electrodes consist of deposited IrO_x films according to various methods described in the literature: sputtering, electrodeposition and thermal methods. El-Giar and Wipf [3] have prepared a microparticles IrO_2 ultramicroelectrode from the anodic oxidation of iridium particles for monitoring pH changes during the oxygen reduction reaction at an iron electrode.

Other metal oxide materials have been considered, but only few works concern manganese dioxide (MnO_2) for a pH sensor application [17]. However, both its low cost and toxicity make it attractive from economic and environmental points of view.

The aim of this work is to study an electrolytic manganese dioxide powder used in alkaline batteries by means of a cavity microelectrode to determine its potentialities as a pH sensor. Besides its low cost, the implementation of a MnO_2 powder-based sensor would avoid the preparation of a film and the reproducibility problems linked to the film formation and the sensor could be easily renewed in case of damaging. A specific attention will be paid to the description of the equilibriums involved at the interface oxide surface|solution, allowing the interpretation of the potential–pH curve in the whole pH range investigated.

2. Experimental

Manganese dioxide powder consisted of an electrolytic-type MnO_2, purchased from Tekkosha and used as received without any further purification. Its physico-chemical characteristics were previously described elsewhere [18]. Redox titration of the initial MnO_2 compound showed that it contains 4 at.% of Mn(III) leading to the following formula $MnO_{1.98}$. The lack of charge due to Mn^{3+} ions in the structure is compensated by the presence of protons which were evidenced by Inelastic Neutron Scattering. As a result, the material contains 4 at.% of MnOOH.

* Corresponding author. Tel.: +33 1 49 78 11 37; fax: +33 1 49 78 11 48..
E-mail address: cachet@icmpe.cnrs.fr (C. Cachet-Vivier).

0039-9140/$ – see front matter © 2010 Elsevier B.V. All rights reserved.
doi:10.1016/j.talanta.2010.05.006

The cavity microelectrode (CME) [19] consisted of a homemade 50 μm in diameter platinum microelectrode. After the sealing of the Pt microwire in a soft glass-tube, the platinum wire was drilled in its centre by laser ablation, forming a cavity of about 40 μm in diameter and 25 μm in depth on the apex of the electrode. The cavity was filled with the MnO_2 powder using the electrode as a pestle [20,21].

Some experiments were performed with a Nafion film as proton-conducting membrane. The coverage of the filled cavity microelectrode with a Nafion coating was performed by two sequential dipping of the electrode (30 s each) in 5 wt.% Nafion in lower aliphatic alcohols and water provided by Aldrich and used as received. The electrode was then dried at 80 °C during 10 min.

The CME was then used as a potentiometric sensor with a saturated calomel electrode (SCE) as reference electrode. Potential variations were recorded at the open circuit potential using a CH Instrument potentiostat suited for the use of microelectrodes. Simultaneous pH measurements were performed with a portable device (Water pH Test 30 – EUTECH Instrument). The pH response of the sensors has not been investigated in buffered solutions, and pH variations were obtained by addition of H_2SO_4 or NaOH at different concentrations.

3. Results and discussion

In the following section, the pH–potential diagrams of a MnO_2 powder are investigated with a CME with and without Nafion membrane as proton-conducting membrane.

3.1. Without Nafion membrane

MnO_2/MnOOH redox system is pH dependent, involving various chemical reactions such as disproportionation of MnOOH in acidic medium [22]. Thus experiments were started first in basic solution and then the acidic media were investigated.

After 24 h immersion in 1 mol L^{-1} KOH solution, the potential variations as a function of the pH of the solution for a CME filled with MnO_2 powder without any Nafion membrane were measured (Fig. 1) starting from a basic solution and lowering the pH by successive addition of acidic solution. The potential–pH curve exhibits two well defined linear domains, the slopes of which are −45.6 mV pH^{-1} (R^2 = 0.999) and −118 mV pH^{-1} (R^2 = 0.998) for pH ranges 7–12.5 and 2–7, respectively.

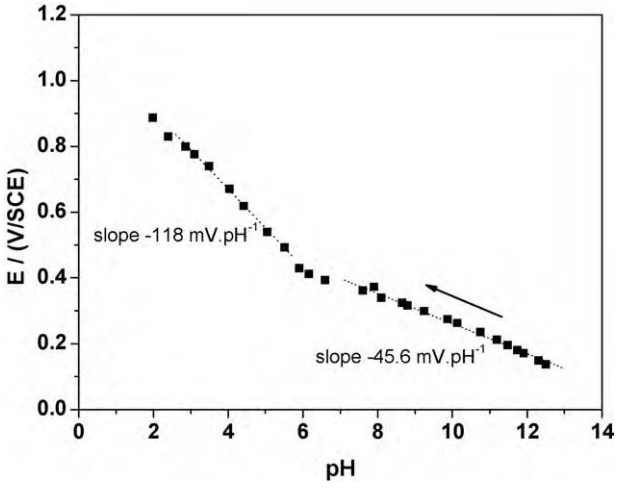

Fig. 1. Potential–pH curve obtained by addition of H_2SO_4 for a CME containing MnO_2 powder without membrane after immersion during 24 h in 1 mol L^{-1} KOH solution.

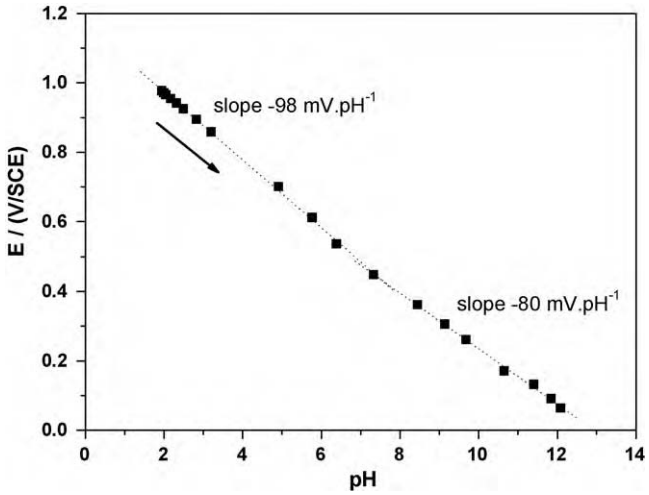

Fig. 2. Potential–pH curve obtained by addition of NaOH for a CME containing MnO_2 powder without membrane after immersion during 24 h in 10^{-2} mol L^{-1} H_2SO_4.

In alkaline media, the manganese oxyhydroxide is known to be a stable species, and the redox equilibrium that takes place is given by Eq. (1):

$$MnO_2 + H^+ + e^- \rightleftharpoons MnOOH \quad (1)$$

allowing the electrode potential, E, to be written as:

$$E = E^0_{MnO_2/MnOOH} + 2.3\frac{RT}{F}\log\left(\frac{a_{MnO_2}}{a_{MnOOH}}\right) + 2.3\frac{RT}{F}\log(a_{H^+}) \quad (2)$$

where $E^0_{MnO_2/MnOOH}$ is the standard redox potential, a_X stands for the activity of the species X, and the other parameters have their usual meaning. From this relationship, the E–pH slope in alkaline solution is −59 mV pH^{-1} (at 298 K).

Conversely, in acidic medium, MnOOH is not stable and disproportionates according to reaction (3):

$$2MnOOH + 2H^+ \rightleftharpoons Mn^{2+} + MnO_2 + 2H_2O \quad (3)$$

In these conditions, Mn^{2+} ions arise from disproportionation and the redox equilibrium to be considered is given by the relationship (4):

$$MnO_2 + 4H^+ + 2e^- \rightleftharpoons Mn^{2+} + 2H_2O \quad (4)$$

Thus, in acidic solution, the MnO_2/Mn^{2+} redox couple governs the potential with an expected slope of −118 mV pH^{-1} (at 298 K).

Thus, the two experimental slopes determined in Fig. 1 clearly indicate that two different electrochemical systems have to be considered. The comparison with theoretical expected slopes suggests that MnO_2/MnOOH is involved in the basic domain (theoretical slope of −59 mV pH^{-1}) whereas MnO_2/Mn^{2+} controls pH variations in the acidic domain (theoretical slope of −118 mV pH^{-1}). It should be mentioned that for the later, the slope compares favorably with the theoretical value. This suggests that the Mn^{2+} activity is constant indicating that those ions remain at the oxide surface. In addition, the measured potentials are in good agreement with the thermodynamic data [22,23].

Fig. 2 shows the evolution of a potential–pH curve when measurements are started in an acidic medium after immersion of the electrode during 24 h in 10^{-2} mol L^{-1} H_2SO_4. This curve shows two linear domains: a slope of −98 mV pH^{-1} (R^2 = 0.999) in the 2–7 pH range and a slope of −80 mV pH^{-1} (R^2 = 0.999) in the 7–12.5 pH range. These values do not match the theoretical values that can be determined from the Nernst's law for the systems MnO_2/MnOOH

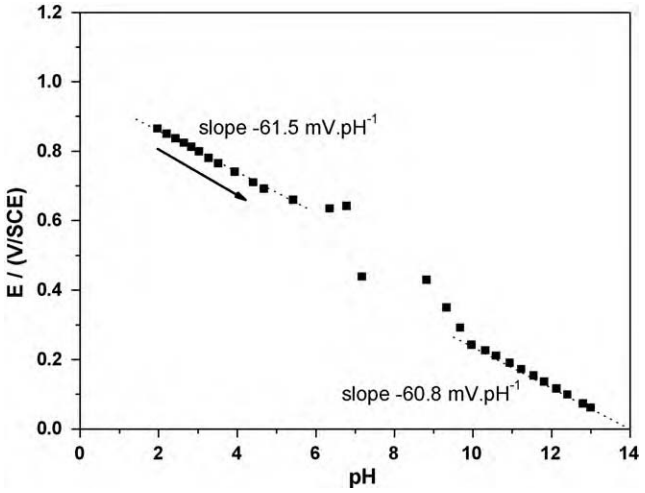

Fig. 3. Potential–pH curve obtained by addition of NaOH for a CME containing MnO_2 powder without membrane after immersion during 24 h in 10^{-2} mol L^{-1} H_2SO_4 and 10^{-1} mol L^{-1} Na_2SO_4.

and MnO_2/Mn^{2+}. Moreover, such differences with theoretical values have already been reported by several authors. Qingwe et al. [17] obtained about -78 mV pH^{-1} and suggested that the main reaction involved in the mechanism is the reaction (5):

$$3MnO_2 + 4H^+ + 4e^- \rightleftharpoons Mn_3O_4 + 2H_2O \quad (5)$$

allowing a slope of -78.9 mV pH^{-1} to be determined. If this redox system can be considered in basic medium, Mn_3O_4 is nevertheless not a stable species in acidic medium in the view of potential–pH diagram [23]. Moreover, Tari and Hirai [24,25] found slopes ranging from -90 to -100 mV pH^{-1} for β-MnO_2. They explained these results with the presence of Mn^{2+} ions arising from the disproportionation of MnOOH according to the reaction (3). This last explanation seems reasonable since we have shown that the potential–pH diagram plotted from alkaline to acidic solution (Fig. 1) was controlled by the MnO_2/Mn^{2+} redox system for acidic pH, so clearly evidencing the presence of Mn^{2+} ions. It can thus be assumed that the Mn^{2+} ions are slowly replaced by Na^+ ions under NaOH addition. As a consequence, the Mn^{2+} concentration progressively decreases at the material surface, and thus the slope is larger than -118 mV pH^{-1}.

This assumption was verified using a CME containing MnO_2 powder immersed during 24 h in a 10^{-2} mol L^{-1} H_2SO_4 solution, in which 10^{-1} mol L^{-1} Na_2SO_4 was added in order to remove the Mn^{2+} ions from the MnO_2 surface. The potential–pH evolution under NaOH addition is shown in Fig. 3. Between pH 2 and 5 and between pH 9 and 13, the curve exhibits two linear domains, the slopes of which are about -60 mV pH^{-1}, that is a value close to the theoretical one for the system MnO_2/MnOOH. In acidic medium, the slope differs from the -98 mV pH^{-1} value obtained when the electrode was immersed only in H_2SO_4 (such a difference in slope was also obtained by Tari and Hirai [26] in presence of different electrolytes). This is in agreement with the removal of all Mn^{2+} ions from the surface. It should also be noticed that the second segment is not in the continuation of the first one, and some erratic points are observed in the pH zone between these two segments. Such a behaviour may be explained by surface effects according to the theory proposed by Tamura et al. [27] and applied more recently by Malloy et al. [28,29].

This theory suggests the presence of two types of sites, acidic sites [≡MnOH(a)] and basic sites [≡MnOH(b)], which undergo dissociation in aqueous medium according to the two following reactions:

$$[\equiv \mathrm{MnOH(a)}] + Na^+ \rightleftharpoons [\equiv MnO^-, Na^+] + H^+ \quad (6)$$

$$[\equiv \mathrm{MnOH(b)}] + H_2O + (1/2)SO_4^{2-} \rightleftharpoons \left[\equiv MnOH_2^+, \left(SO_4^{2-}\right)_{1/2}\right] + OH^- \quad (7)$$

The thermodynamic constants for each equilibrium, K_a and K_b, respectively, were determined from acid–base titrations [27–29] of a MnO_2 suspension in NaOH solution. Tamura et al. [27] found pK_a values between 5.1 and 5.9, and pK_b values between 9.6 and 10.8 depending on the ionic strength. Malloy et al. [28,29] determined pK_a = 6 and pK_b = 9.3 for another type of electrolytic MnO_2. These acid–base titration curves show an equivalence point between 5 and 9, corresponding to the instability potential domain observed in Fig. 3 and to neutralization end point of predominant species present in acidic medium [≡MnOH(a)], and $[\equiv MnOH_2^+, (SO_4^{2-})_{1/2}]$. In basic medium, after the neutralization, the predominant species are then $[\equiv MnO^-, Na^+]$ arising from dissociation of acid groups and [≡MnOH(b)].

Finally, the potential–pH evolutions in the experiments shown in Figs. 1 and 2 are mainly governed by the disproportionation reaction of MnOOH leading to the formation of Mn^{2+} ions, which are slowly exchanged with other cations (H^+, Na^+, ...) and can undergo precipitation reactions. When Mn^{2+} ions are completely removed from the MnO_2 surface, the main effects influencing the potential–pH evolution are then acid–base properties, arising from the presence of acidic and basic sites [≡MnOH(a)] and [≡MnOH(b)], respectively.

In all cases, chemical reactions or surface effects induce complex evolutions of the potential–pH curves at the MnO_2 electrode. Such a behaviour is not suited for a pH sensor application. In the following paragraph, we describe an improvement of this electrode by covering the apex of the electrode with a Nafion membrane, which can also act as a protection of the sensor surface in complex matrices.

3.2. With a Nafion membrane

3.2.1. Potential–pH response

The Nafion membrane was initially used as a permselective ionomer coating for attenuating the effect of the anionic redox species on metal oxide electrode similarly to iridium oxide pH sensors [30,31]. Fig. 4 shows the evolution of the potential–pH curve under addition of NaOH (black squares) and further addition of H_2SO_4 (red circles) for a MnO_2–CME coated by a Nafion mem-

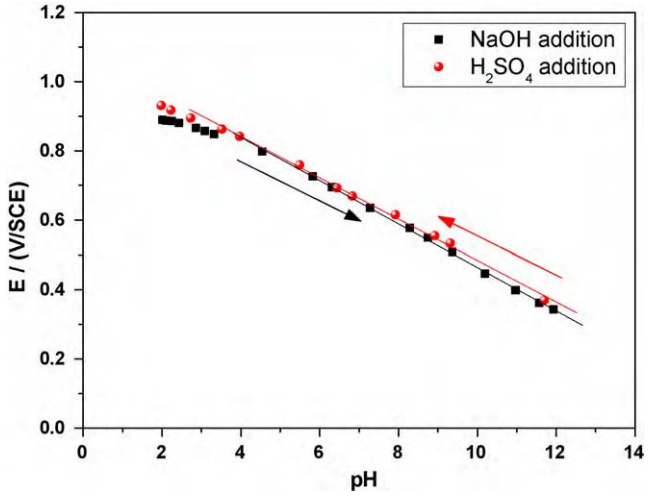

Fig. 4. Potential–pH curves obtained by addition of NaOH (■) and further addition of H_2SO_4 (●) for a CME containing MnO_2 powder coated by a Nafion membrane. (For interpretation of the references to color in this figure legend, the reader is referred to the web version of the article.)

brane. The two potential–pH curves vary linearly with slopes close to −60 mV pH^{-1} and with good correlation factors (−62.6 mV pH^{-1}, R^2 = 0.999 under NaOH addition, −59.7 mV pH^{-1}, R^2 = 0.997 under H_2SO_4 addition). These slopes were calculated by neglecting points around pH 2.

Processes appear much simpler with such a sensor than in the absence of Nafion membrane, indicating that no dissolution reaction, neither precipitation reaction nor oxide formation occurs. In that case, MnO_2 constitutes the reference material, and the half cell that account for pH variations is MnO_2/Mn^{2+}||internal H^+||Nafion membrane||external H^+. As a result, only MnO_2/Mn^{2+} redox couple has to be considered since the Nafion solution used for preparing the membrane is a superacid allowing the formation of a small amount of Mn^{2+} ions due to disproportionation of MnOOH.

The potential of such an electrode may be written as

$$E = E_{ref} - 2.3\frac{RT}{F}pH_{ext} \quad (8)$$

where E_{ref} is the potential of the reference system in the internal solution (including the inner membrane interface) and pH_{ext} is the pH value of the external solution. The expected slope of the E–pH curve is then −60 mV pH^{-1}, which compares the experimental slope determined in Fig. 4. Moreover, such a sensor description is in good agreement with the literature data in which MnO_2 was already used as internal reference for pH sensors [32,33].

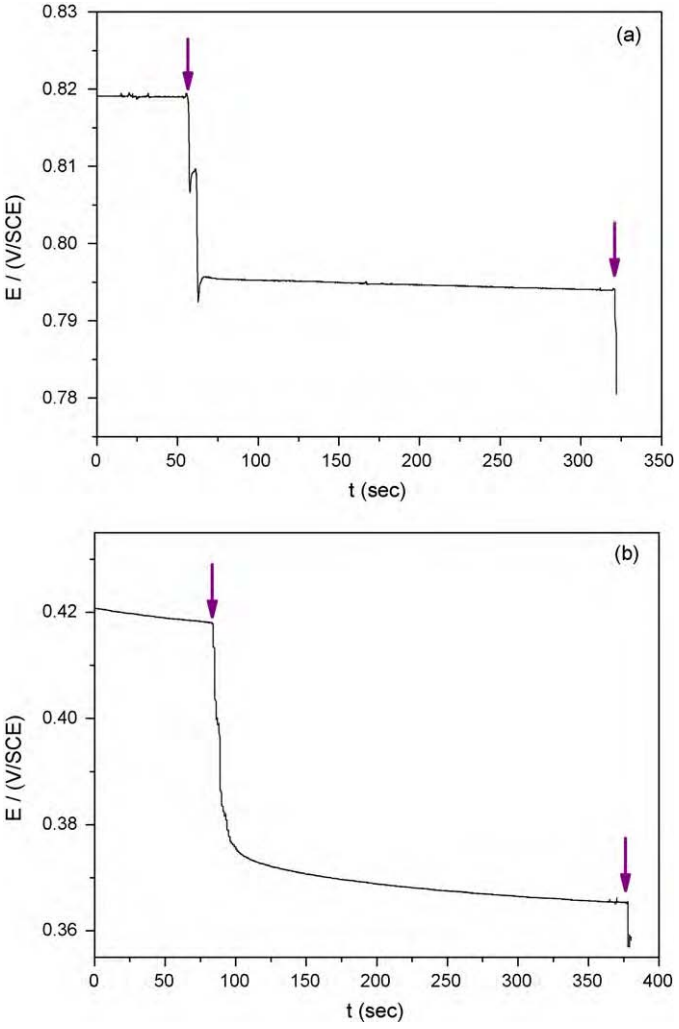

Fig. 5. Time response of the MnO_2–CME sensor coated by a Nafion membrane upon the addition of NaOH solution (indicated by arrows). (a) Initial pH 4.4; and (b) initial pH 10.7.

In addition, the E–pH evolution curve upon H_2SO_4 addition is very similar to the one obtained during NaOH addition for both the slope and the potential values, indicating a good reversibility of the proton adsorption. With such a sensor, the pH range that exhibits a linear response is 2–12, which is very similar to the domain obtained with other materials [3,30,34].

3.2.2. Time response of the MnO_2/Nafion coating electrode

Fig. 5 compares potential response–time curves for a Nafion coated MnO_2–CME obtained by random additions of NaOH solution. As already observed for IrO_2-coated pH sensors, the time response is pH dependant [30,31,34]. It requires about 35 s to reach 95% of the stabilized potential when the experiment is performed in acidic medium from an initial pH of 4.4 with a pH step, ΔpH, of 0.4 (Fig. 5a), and requires 74 s in basic medium when the experiment is performed from an initial pH of 10.7 with ΔpH = 0.9 (Fig. 5b). Moreover, most of the potential change occurs in the very first seconds showing that this sensor is suited for monitoring fast pH change. In addition, the sensitivity of the sensor was about one tenth of pH unit range in both acidic and basic solutions. The stability of the sensors is good in as much as sensors are soaked in acidic solution for storage. After two weeks, the potential drift was about 10 mV (corresponding to ΔpH = 0.17), indicating that a calibration procedure has to be performed before the use of the sensor, but no change of the sensitivity or of the time response could have been evidenced. El-Giar and Wipf [3] reported an aging effect of IrO_x microparticle pH sensor after one week, but the sensor construction was done without any coating. In our case, the Nafion coating is assumed to act as a protective layer for the manganese oxide.

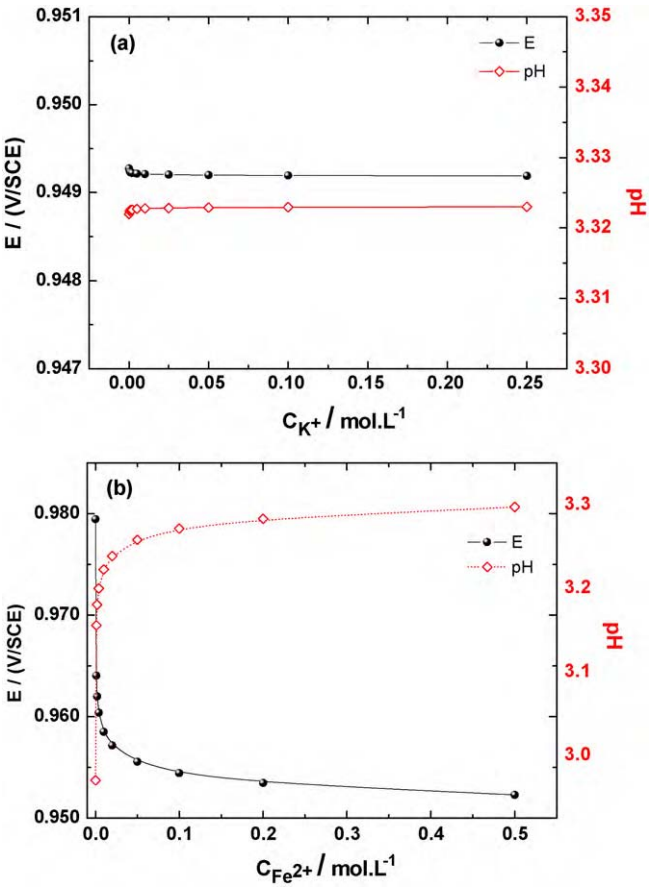

Fig. 6. Potential (●) and pH variations (◇) for the MnO_2/Nafion membrane CME as a function of concentration of added ion: (a) K^+, and (b) Fe^{2+} at pH ~ .

3.2.3. Electrode selectivity

Fig. 6 shows the selectivity studies performed on K^+ ions (Fig. 6a) and for a redox species, Fe^{2+} (Fig. 6b) at pH of ca. 3.3. These curves are plotted with a double vertical scale, the right scale corresponding to pH values calculated from the measured potential (left scale) and the calibration curve presented in Fig. 4. Fig. 6a shows that K^+ cations had no adverse effect on the potential response of the pH sensor since the variations observed are smaller than 0.01 pH unit that is in the range of experimental error. In the case of Fe^{2+} ions, interference was observed depending on the concentration. For a 10^{-3} mol L^{-1} Fe^{2+} solution (Fig. 6b), the potential variation is equal to 1.6% (corresponding to a 0.18 pH unit change). Further additions induce a progressive potential decrease with a 2.7% variation, corresponding to a 0.3 pH unit change. This can be explained by competition between Fe^{2+} ions and H^+ ions: in fact some authors [35] have shown than Nafion membrane can concentrate small amount of iron ions by ion-exchange reaction in acidic media.

4. Conclusion

The potentiometric response of an electrolytic manganese dioxide was examined by means of a cavity microelectrode (CME). It has been shown that the potential–pH curves strongly depend on the initial conditions of the experiment, and different potentiometric curves are obtained when measurements are started in acidic or in basic solution. In both cases, two linear segments with different slopes that could have been evidenced and interpreted by the disproportionation of MnOOH species, leading to the formation of Mn^{2+} ions on the MnO_2 surface. Such a complex evolutions is not suitable for pH sensor application. However when the tip of the electrode is coated by a Nafion membrane, the potentiometric response of the sensor shows a unique slope close to the theoretical value of -60 mV pH^{-1}. In addition, short time responses to step pH variations in both acidic and basic solutions, and good sensitivity were obtained. This Nafion coated MnO_2–CME could be used as pH sensor for localized measurements with the advantage to be easily renewable in few minutes by filling the cavity with fresh powder. This compare favorably with usual electrodeposited iridium oxide thin-film microsensors for which the preparation procedure is longer. The use of cavity microelectrode as a tool for pH sensing appears to be a promising way. It offers the possibility of using various types of metal oxides or other materials. Works are under progress for the study of pH variation associated with localized corrosion of iron and steels in acidic and neutral solution.

References

[1] B.R. Horrocks, M.V. Mirkin, D.T. Pierce, A.J. Bard, G. Nagy, K. Toth, Anal. Chem. 65 (1993) 1213.
[2] E. Klusmann, J.W. Schultze, Electrochim. Acta 48 (2003) 3325.
[3] E.E-D.M. El-Giar, D.O. Wipf, J. Electroanal. Chem. 609 (2007) 147.
[4] D.O. Wipf, F. Ge, T.W. Spaine, J.E. Baur, Anal. Chem. 72 (2000) 4921.
[5] H. Tanabe, K. Togashi, T. Misawa, U. Kamachi Mudali, J. Mater. Sci. Lett. 17 (1998) 551.
[6] K. Murase, T. Honda, T. Hirato, Y. Awakura, Metall. Mater. Trans. B 29 (1998) 1193.
[7] T. Honda, K. Murase, T. Hirato, Y. Awakura, J. Appl. Electrochem. 28 (1998) 617.
[8] A. Richter, G. Paschew, S. Klatt, J. Lienig, K.-F. Arndt, H-J.P. Adler, Sensors 8 (2008) 561.
[9] M.L. Pourciel-Gouzy, W. Sant, I. Humenyuk, L. Malaquin, X. Dollat, P. Temple-Boyer, Sens. Actuator B 103 (2004) 247.
[10] J. Ji, Z. Rosenzweig, Anal. Chim. Acta 397 (1999) 93–102.
[11] J. Hendrikse, W. Olthuis, P. Bergveld, Sens. Actuator B 53 (1998) 97.
[12] J.M. Zhang, C.J. Lin, Z.D. Feng, Z.W. Tian, J. Electroanal. Chem. 452 (1998) 235.
[13] H. Suzuki, H. Shiroishi, S. Sasaki, I. Karube, Anal. Chem. 71 (1999) 5069.
[14] M. Wang, S. Yao, M. Madou, Sens. Actuator B 81 (2002) 313.
[15] A.N. Bezbaruah, T.C. Zhang, Ann. Chem. 74 (2002) 5726.
[16] I.A. Ges, B.L. Ivanov, D.K. Schaffer, E.A. Lima, A.A. Werdich, F.J. Baudenbacher, Biosens. Bioelectron. 21 (2005) 248.
[17] L. Qingwe, W. Yiming, L. Guoan, Sens. Actuator B: Chem. 59 (1999) 42.
[18] F. Fillaux, C. Cachet, H. Ouboumour, J. Tomkinson, C. Levy-Clément, L.T. Yu, J. Electrochem. Soc. 140 (1993) 585.
[19] V. Vivier, C. Cachet-Vivier, C.S. Cha, J.-Y. Nedelec, L.T. Yu, Electrochem. Commun. 2 (2000) 180.
[20] V. Vivier, C. Cachet-Vivier, B.L. Wu, C.S. Cha, J.-Y. Nedelec, L.T. Yu, Electrochem. Solid-State Lett. 2 (1999) 385.
[21] C Cachet-Vivier, V. Vivier, J.-Y. Nedelec, C.S. Cha, L.T. Yu, Electrochim. Acta 47 (2001) 181.
[22] J.P. Brenet, J.P. Gabano, J. Reynaud, Electrochim. Acta 8 (1963) 207.
[23] Atlas d'équilibres électrochimiques, Marcel Pourbaix, Gauthier-Villars & Cie Editeur, Paris, 1963.
[24] I. Tari, T. Hirai, Electrochim. Acta 26 (1981) 1657.
[25] I. Tari, T. Hirai, Electrochim. Acta 27 (1982) 149.
[26] I. Tari, T. Hirai, Electrochim. Acta 27 (1982) 235.
[27] H. Tamura, T. Oda, M. Nagayama, R. Furuichi, J. Electrochem. Soc. 136 (10) (1989) 2782.
[28] A.P. Malloy, G.J. Browning, S.W. Donne, J. Colloid Interface Sci. 285 (2005) 653.
[29] A.P. Malloy, S.W. Donne, J. Colloid Interface Sci. 320 (2008) 210.
[30] P.J. Kinlen, J.E. Heider, D.E. Hubbard, Sens. Actuator B 22 (1994) 13.
[31] S.A.M. Marzouk, Anal. Chem. 75 (2003) 1258.
[32] L. Zerroual, L. Telli, Sens. Actuator B 24–25 (1995) 741.
[33] L. Telli, B. Brahimi, A. Hammouche, Solid State Ionics 128 (2000) 255.
[34] S.A.M. Marzouk, S. Ufer, R.P. Buck, T.A. Johnson, L.A. Dunlap, W.E. Cascio, Anal. Chem. 70 (1998) 5054.
[35] P. Ugo, F. Cavalieri, D. Rudello, L.M. Moretto, E. Argese, Sensors 1 (2001) 102.